An Error-Checking Method for Delta-Sigma Analog-to-Digital Converters Employing *M*th-Order Sinc Filters

Travis C. Mallett
Schweitzer Engineering Laboratories, Inc.

Original edition released October 2017

An Error-Checking Method for Delta-Sigma Analog-to-Digital Converters Employing *M*th-Order Sinc Filters

Travis C. Mallett, *Schweitzer Engineering Laboratories, Inc.*

Abstract—**Oversampling analog-to-digital converters often employ sinc-shaped filters for noise shaping and decimation. These digital filters exhibit a limited slew rate and other deterministic characteristics. By knowing these characteristics, consecutive samples of an analog-to-digital converter can be analyzed to verify fundamental data integrity. If excursions are observed, it is likely that some corruption of the digitized data has occurred and appropriate action can be taken. This paper develops a patent-pending error-checking method for analog-to-digital converters and analyzes the transfer function for an *M*th-order sinc-shaped filter with an oversample ratio of *N*. It also solves the impulse and step responses of an arbitrary sinc filter and discusses several properties of the impulse and step responses via theorems with corresponding proofs. It proves that, for a sinc filter reporting values every *N*th term referred to the input rate, there is a maximum change in value between any two consecutive output samples. The paper calculates the maximum change in value for a sinc filter of an arbitrary order and decimation rate. Finally, additional characteristics of limited slew rates are discussed, and a three-limit error-checking scheme is developed for the specific case of a third-order modulator with an oversample ratio of 64. Test results using a commercially available analog-to-digital converter are presented, which indicate that the error-checking scheme is useful for detecting catastrophic data converter failures.**

Index Terms—**Analog-to-digital conversion, digital filters, fault detection, sigma-delta modulation.**

I. Introduction

As digital technology continues to permeate our modern world, ever more important decisions are made by intelligent electronic devices (IEDs). IEDs often employ analog-to-digital converters (ADCs) as their primary, if not sole, window into the analog world and often place utmost trust on ADC conversion results. ADC conversion failures in mission-critical applications are a dominant concern in contemporary electronic design.

ADC integrity has traditionally been verified by several methods, including multiplexing a known voltage (e.g., ground or a reference voltage) [1], injecting a test tone [2], or implementing voting methods with redundant cross-checking ADCs [3]. IEDs that require significant accuracy and precision may use oversampling ADCs with a delta-sigma (ΔΣ) topology. These ADCs employ digital filters for noise shaping and decimation [4]. Sinc-shaped filters are a popular choice for ΔΣ applications. However, these digital filters often introduce appreciable latency, and this latency is often seen as a primary disadvantage of ΔΣ ADCs [5].

Because of these digital filters, traditional error-checking methods (e.g., sampling the ground voltage) are often not possible for ΔΣ ADCs without adding significant complexity and latency to the data acquisition system. This paper develops a patent-pending error-checking method that capitalizes on the limited slew rate properties of the internal sinc-shaped filters, also known as simply sinc filters or cascaded integrator-comb (CIC) filters [6] [7]. When subjected to a step input (u[n]), sinc filters exhibit a nonzero finite rise time (dV/dn), as shown in Fig. 1. This rise time represents the fastest possible slew rate of the filter. By comparing the difference between every pair of consecutive samples being reported by the ΔΣ converter, a system can have some confidence that severe digital corruption has not occurred.

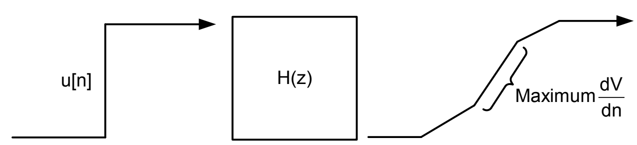

Fig. 1. The step response of a sinc filter with transfer function H(z) has a finite, nonzero rise time or a maximum dV/dn if the output is given in volts.

For example, a commercially available ΔΣ ADC suffered a severe overvoltage event on its inputs. The ADC immediately began producing the data shown in Fig. 2. These data, according to the method presented in this paper, can be detected as characteristic of a faulty ADC because several sets of data points exceed the fastest slew rate possible from the ADC's internal sinc filter. A system with no knowledge of the ADC's internal characteristics can react to faulty data with a potentially catastrophic action (e.g., tripping a breaker). If, however, the system recognizes that the data do not conform to the mathematical characteristics of a properly working ΔΣ ADC, the data can be disregarded or other appropriate action taken.

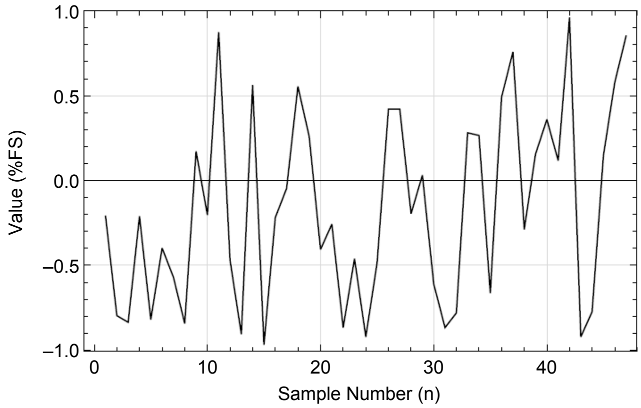

Fig. 2. Digital output referenced to the full scale of a commercially available ΔΣ after an overvoltage stress condition (%FS is the percent of full-scale ADC range). In a properly working ΔΣ ADC, the difference between consecutive samples is limited by the mathematical properties of the internal sinc filter. Several samples in this data set exceed these limitations, indicating a faulty ADC.

In the development of the error-checking method, this paper analyzes the transfer function for an *M*th-order sinc filter with an oversample ratio of *N* and solves the impulse and step responses of an arbitrary sinc filter. Several properties of the impulse and step responses are discussed via theorems with corresponding proofs.

The paper proves that for a sinc filter reporting values every *N*th term referred to the input rate, there is a maximum change in value between any two consecutive output samples. The maximum change in value for a sinc filter of arbitrary order and decimation rate is calculated.

Finally, the paper discusses additional characteristics of limited slew rates and develops a three-limit error-checking scheme for the specific case of a third-order modulator with an oversample ratio of 64. Test results using a commercially available ADC are presented, which indicate that the calculations conform closely to physical reality.

II. Algebraic Expansion of Sinc Filter Transfer Function

Begin with the z-domain transfer function of an *M*th-order sinc filter with an oversample ratio of *N*, as shown in (1):

$$H(z)=\left[\frac{1-z^{-N}}{1-z^{-1}}\right]^{M} \tag{1}$$

The expression for a first-order sinc filter resembles the closed-form solution to a finite geometric series [8], as shown in (2).

$$\frac{1-z^{-N}}{1-z^{-1}}=1+z^{-1}+z^{-2}+\ldots+z^{-(N-1)} \tag{2}$$

Thus, the *M*th-order sinc filter can be written as (3).

$$H(z)=\left(1+z^{-1}+z^{-2}+\ldots+z^{-(N-1)}\right)^{M} \tag{3}$$

Expand this into the form shown in (4), where each C_a, $a \in [0, M(N-1)]$ is a coefficient resulting from the expansion.

$$\begin{aligned} H(z)&=C_0+C_1z^{-1}+\ldots+C_{M(N-1)}z^{-M(N-1)} \\ &=\sum_{a=0}^{M(N-1)} C_a z^{-a} \end{aligned} \tag{4}$$

This is a special case of the classic multinomial expansion problem. The general solution for multinomial expansion is given by the multinomial theorem [8], the computation of which usually requires recursive summations in which each coefficient depends on the preceding ones.[1] A nonrecursive, closed-form solution for each coefficient was first solved by de Moivre in 1711 [11]. In keeping with the notation of the binomial theorem, the expansion is notated as shown in (5).

$$\left(1+x+x^2+\ldots+x^q\right)^L=\sum_{a\ge 0}\binom{L}{a}_q x^a \tag{5}$$

Note that $\binom{L}{a}_1=\binom{L}{a}$ (the usual binomial coefficient) and $\binom{L}{a}_q=0$ for all $a > qL$. The multinomial coefficients[2] are shown in (6).

$$\binom{L}{a}_q=\sum_{j=0}^{\left\lfloor \frac{a}{(q+1)} \right\rfloor}(-1)^j\binom{L}{j}\binom{a-j(q+1)+L-1}{L-1} \tag{6}$$

Writing (6) in terms of the sinc filter yields the coefficients of (4), as shown in (7).

$$C_a=\binom{M}{a}_{N-1} \tag{7}$$

Summarizing and writing the completely expanded general sinc filter transfer function[3] results in (8).

$$\begin{aligned} H(z)&=\left[\frac{1-z^{-N}}{1-z^{-1}}\right]^{M} \\ &=\left(1+z^{-1}+z^{-2}+\ldots+z^{-(N-1)}\right)^{M} \\ &=C_0+C_1z^{-1}+\ldots+C_{M(N-1)}z^{-M(N-1)} \\ &=\sum_{j=0}^{M(N-1)}\binom{M}{j}_{N-1}z^{-j} \\ &=\sum_{j=0}^{M(N-1)}\sum_{k=0}^{\left\lfloor \frac{j}{N} \right\rfloor}\left\{(-1)^k\binom{M}{k}\bullet\binom{j-kN+M-1}{M-1}z^{-j}\right\} \end{aligned} \tag{8}$$

[1] See the so-called Villareal Method for an explicit recursive formula in [9] as well as the method developed by Leonhard Euler in [10].

[2] Arrays of multinomial coefficients are often referred to in the literature as Pascal's pyramids or generalized Pascal triangles. Here $\binom{L}{a}_q$ is referred to simply as a multinomial coefficient.

[3] Eugene Hogenauer, who is credited with inventing the CIC filter, arrives at the same transfer function expansion using similar techniques in [12].

III. Properties of Sinc Filter Transfer Function

This section provides several theorems and corresponding proofs based on the prior discussion. These properties are useful for understanding the nature of the sinc filter and are necessary to derive the maximum dV/dt relationship described in Section I.

A. Theorem 3.1

Let h[n] = $\mathcal{Z}^{-1}$ {H(z)} be the impulse response of an *M*th-order sinc filter with an oversampling ratio of *N* and the transfer function shown in (9).

$$H(z)=\left[\frac{1-z^{-N}}{1-z^{-1}}\right]^{M} \tag{9}$$

The value of h[n] for any sample $n \in \mathbb{N}$ is precisely equal to a corresponding multinomial coefficient ($\mathbb{N}$ is the set of natural numbers, i.e., positive integers). Theorem 3.1 is shown in (10).

$$h[n]=\binom{M}{n}_{N-1} \tag{10}$$

B. Theorem 3.1 Proof

Let $\mathcal{Z}^{-1}$ be the inverse z-transform operator, as shown in (11).

$$\mathcal{Z}^{-1}: H(z)\rightarrow h[n] \tag{11}$$

The impulse response h[n] of a discrete-time system is defined as the inverse z-transform of the system's transfer function H(z). Begin with H(z), as shown in (12).

$$\begin{aligned} H(z)&=\left[\frac{1-z^{-N}}{1-z^{-1}}\right]^{M} \\ &=\left(1+z^{-1}+z^{-2}+\ldots+z^{-(N-1)}\right)^{M} \\ &=C_0+C_1z^{-1}+\ldots+C_{M(N-1)}z^{-M(N-1)} \\ &=\sum_{j=0}^{M(N-1)}\binom{M}{j}_{N-1}z^{-j} \end{aligned} \tag{12}$$

Then take the inverse z-transform:

$$\begin{aligned} h[n]&=\mathcal{Z}^{-1}\{H(z)\} \\ &=\mathcal{Z}^{-1}\left\{\sum_{j=0}^{M(N-1)}\binom{M}{j}_{N-1}z^{-j}\right\} \\ &=\sum_{j=0}^{M(N-1)}\mathcal{Z}^{-1}\left\{\binom{M}{j}_{N-1}z^{-j}\right\} \\ &=\sum_{j=0}^{M(N-1)}\binom{M}{j}_{N-1}\delta[n-j] \end{aligned} \tag{13}$$

(where δ[x] is the discrete-time unit impulse)

$$\begin{aligned} &=\sum_{j\neq n}\binom{M}{j}_{N-1}\delta[n-j]+\binom{M}{n}_{N-1}\delta[n-n] \\ &=\binom{M}{n}_{N-1} \quad \blacksquare \end{aligned}$$

C. Theorem 3.2

Let h[n] = $\mathcal{Z}^{-1}$ {H(z)} be the impulse response of an *M*th-order sinc filter with an oversampling ratio of *N* and transfer function (9). The impulse response h[n] exhibits time-reflective symmetry about (14).

$$n=\frac{M(N-1)}{2} \tag{14}$$

This time-reflective symmetry property of the impulse response can be stated as (15).

$$h\left[\frac{M(N-1)}{2}+a\right]=h\left[\frac{M(N-1)}{2}-a\right] \tag{15}$$

Given Theorem 3.1, (15) can be rewritten as (16) (Theorem 3.2).

$$\forall a\in\mathbb{N}:\binom{M}{\frac{M(N-1)}{2}+a}_{N-1}=\binom{M}{\frac{M(N-1)}{2}-a}_{N-1} \tag{16}$$

D. Theorem 3.2 Proof

The property shown in (17) is already well-established [11].

$$\binom{L}{a}_{q}=\binom{L}{qL-a}_{q} \tag{17}$$

Therefore, the proof of Theorem 3.2 is as shown in (18).

$$\begin{aligned} \binom{M}{\frac{M(N-1)}{2}+a}_{N-1}&=\binom{M}{M(N-1)-\left(\frac{M(N-1)}{2}+a\right)}_{N-1} \\ &=\binom{M}{\frac{M(N-1)}{2}-a}_{N-1} \quad \blacksquare \end{aligned} \tag{18}$$

E. Theorem 3.3

Let h[n] = $\mathcal{Z}^{-1}$ {H(z)} be the impulse response of an *M*th-order sinc filter with an oversampling ratio of *N* and transfer function (9). The impulse response $h[n] \geq 0 \ \forall\ n \in \mathbb{N}$ (Theorem 3.3).

F. Theorem 3.3 Proof

Visiting the geometric series form of H(z) in (3) and applying the Multinomial Theorem [8] results in (19):

$$H(z)=\sum_{k_1+\ldots+k_{N-1}=M}\binom{n}{k_1,k_2,\ldots,k_{N-1}}\prod_{1\leq t\leq N-1}z^{-k_t\cdot t} \tag{19}$$

where (20) is a multinomial coefficient.

$$\binom{n}{k_1,k_2,\ldots,k_{N-1}}=\frac{n!}{k_1!k_2!\ \ldots k_{N-1}!} \tag{20}$$

Inspection of (20) shows that the multinomial coefficients are always nonnegative for $n,k_i \in \mathbb{N}\ \forall\ i \in \mathbb{N}$. Based on Theorem 3.1, this results in (21).

$$h[n]\geq 0\ \forall\ n\in\mathbb{N} \ \blacksquare \tag{21}$$

G. Definition

Call a polynomial $A(x) = a_0 + a_1x + a_2x_2 + \cdots + a_nx_n$ unimodal if there is some *t* such that for $i < j \leq t$, $a_i \leq a_j$, and for $t \le i < j$, $a_i \ge a_j$. In other words, the coefficients rise monotonically to a maximum and then decrease monotonically. Call the polynomial A(x) symmetric if for all i, $a_i = a_{n-i}$.

H. Lemma 3.4

If A(x) and B(x) are two symmetric unimodal polynomials, then A(x)B(x) is a symmetric unimodal polynomial.[4]

I. Lemma 3.4 Proof

Begin with (22) and (23).

$$\begin{aligned} A(x) &= \sum_{i=0}^{m} a_i x^i \\ B(x) &= \sum_{n=0}^{n} b_j x^j \end{aligned} \tag{22}$$

$$\begin{aligned} r &= \left\lfloor \frac{m}{2} \right\rfloor \\ s &= \left\lfloor \frac{n}{2} \right\rfloor \end{aligned} \tag{23}$$

Then rewrite the polynomials from (22) in the form shown in (24).

$$\begin{aligned} A(x) &= \sum_{i=0}^{r} \left(a_i - a_{i-1}\right)\left(x^i + x^{i+1} + \ldots + x^{m-i}\right) \\ B(x) &= \sum_{j=0}^{r} \left(b_j - a_{j-1}\right)\left(x^j + x^{j+1} + \ldots + x^{m-j}\right) \end{aligned} \tag{24}$$

This results in (25).

$$\begin{aligned} &A(x)B(x) = \\ &\sum_{i=0}^{r}\sum_{j=0}^{s} \left(a_i - a_{i-1}\right)\left(b_j - b_{j-1}\right) \bullet \left(x^i + \ldots + x^{m-i}\right)\left(x^j + \ldots + x^{n-j}\right) \end{aligned} \tag{25}$$

Note that each term of this sum is a symmetric, unimodal polynomial centered around $x^{(m+n)/2}$. Therefore, the sum A(x)B(x) itself is a symmetric, unimodal polynomial centered around $x^{(m+n)/2}$, as desired. ■

J. Theorem 3.5

Let $h[n] = \mathcal{Z}^{-1}\{H(z)\}$ be the impulse response of an *M*th-order sinc filter with an oversampling ratio of *N* and transfer function (9). The impulse response h[n] monotonically rises to a global maximum centered at M(N – 1)/2, as shown in (26) (Theorem 3.5)

$$\mathrm{Max}\{h[n]\} = h\left[\frac{M(N-1)}{2}\right] \tag{26}$$

K. Theorem 3.5 Proof

Referring to (3), $(1 + z^{-1} + z^{-2} + \cdots + z^{-(N-1)})$ is a unimodal, symmetric polynomial. Applying Lemma 3.4 M − 1 times shows that H(z) is also a unimodal, symmetric polynomial. Furthermore, the symmetry is located around M(N − 1)/2, as expected by Theorem 3.2. ■

[4] Lemma 3.4 is a well-known result in combinatorics and is stated and proved in [13].

L. Theorem 3.6

Begin with (27) as the step response[5] of an *M*th-order sinc filter with an oversampling ratio of *N* and transfer function (9).

$$H[n,a] = \mathcal{Z}^{-1}\left\{H(z)\frac{z^{-a}}{1-z^{-1}}\right\} \tag{27}$$

Equation (28) therefore holds (Theorem 3.6).

$$H[n,a] = \sum_{j=0}^{n} \binom{M}{j-a}_{N-1} \tag{28}$$

M. Theorem 3.6 Proof

Begin with (29).

$$\begin{aligned} H[n,a] &= \mathcal{Z}^{-1}\left\{H(z)\frac{z^{-a}}{1-z^{-1}}\right\} \\ &= \mathcal{Z}^{-1}\{H(z)\} \mathcal{Z}^{-1}\left\{\frac{1}{1-z^{-1}}\right\} \mathcal{Z}^{-1}\{z^{-a}\} \end{aligned} \tag{29}$$

Rewrite the equation as a convolution in discrete time, as shown in (30).

$$= h[n] * u[n] * \delta[n-a] \tag{30}$$

Express the convolution as a sum [14], as shown in (31).

$$\begin{aligned} &= \left(\sum_{k=-\infty}^{\infty} u[k]h[n-k]\right) * \delta[n-a] \\ &= \left(\sum_{k=0}^{\infty} h[n-k]\right) * \delta[n-a] \end{aligned} \tag{31}$$

Substitute Theorem 3.1 into (31), as shown in (32).

$$\begin{aligned} &= \left(\sum_{k=0}^{\infty} \binom{M}{n-k}_{N-1}\right) * \delta[n-a] \\ &= \left(\sum_{k=0}^{n} \binom{M}{n-k}_{N-1}\right) * \delta[n-a] \\ &= \left(\sum_{j=0}^{n} \binom{M}{j}_{N-1}\right) * \delta[n-a] \end{aligned} \tag{32}$$

Apply the convolution with impulses [15], as shown in (33).

$$= \sum_{j=0}^{n-a} \binom{M}{j}_{N-1} = \sum_{j=0}^{n} \binom{M}{j-a}_{N-1} \quad ■ \tag{33}$$

N. Theorem 3.7

Begin with (34) as the step response of an *M*th-order sinc filter with an oversampling ratio of *N* and transfer function (9).

$$H[n] = \mathcal{Z}^{-1}\left\{H(z)\frac{1}{1-z^{-1}}\right\} \tag{34}$$

Equation (35) holds (Theorem 3.7).

$$\lim_{n\to\infty} H[n] = N^M \tag{35}$$

Furthermore, the step response H[n] settles when the time value is n = M(N − 1).

[5] Note that traditionally a unit step function in the z-domain is simply $1/(1 - z^{-1})$. However, because the input to a sinc filter is at a higher sample rate than the output after decimation, the "step response" of the sinc filter changes depending on where the transient input occurs in a "conversion cycle" (*N* samples). Therefore, a delay of *a* samples (z^{-a} in the z-domain) is included for purposes shown later in this document.

O. Theorem 3.7 Proof

Based on Theorem 3.6, (36) is the sum of all multinomial coefficients.

$$\lim_{n\to\infty} H[n] = \lim_{n\to\infty} \sum_{j=0}^{n} \binom{M}{j}_{N-1} \tag{36}$$

Note that $\binom{M}{n}_{N-1} = 0$ for n > M(N – 1).

Applying the results from Theorem 3.6 results in (37).

$$\begin{aligned} H(z) &= \sum_{j=0}^{M(N-1)} \binom{M}{j}_{N-1} z^{-j} \\ &= \left(1 + z^{-1} + \ldots + z^{-N-1}\right)^{M} \end{aligned} \tag{37}$$

Substituting $z^{-a} = 1$ for all a immediately demonstrates (38).

$$\sum_{j=0}^{M(N-1)} \binom{M}{j}_{N-1} = N^{M} \tag{38}$$

Also, note (39).

$$\binom{M}{j}_{N-1} = 0 \ \forall \ j > M(N-1) \tag{39}$$

The step response settles to $H[n] = N^M$ at $n = M(N - 1)$ ■.

P. Normalized Step Response Definition

Using the result of Theorem 3.7, define the normalized step response of a sinc filter, as shown in (40).

$$H_{\|H\|}[n,a] = \frac{1}{N^{M}} \sum_{j=0}^{n} \binom{M}{j-a}_{N-1} \tag{40}$$

That is, the step response settles to 1 and the intermediate values can be viewed as percentages of the final value (%FS). From here on, all step responses are assumed to be normalized unless otherwise noted. Additionally, no special notation is used to indicate normalization: $H_{\|H\|}[n,a] \equiv H[n,a]$.

IV. Decimated Sinc Filter With Decimation Ratio *N*

Sinc filters are primarily used for decimation in oversampling ADCs. Usually, the output of the sinc filter is not reported at the modulator rate but rather is reported every *N* samples. A physical implementation of a first-order sinc filter is simply a counter that implements an accumulate-and-dump scheme [6], [16], [17]. Thus, a sinc filter and decimator may be one and the same and perform filtering and decimation simultaneously. Fig. 3 shows the step response of a third-order sinc filter decimated every 64 samples at the modulator rate (M = 3, N = 64).

Henceforth, "decimated sinc filter" will mean simply a sinc filter whose output is taken every *N* samples, where *N* is the oversample ratio. Thus, the step response of a decimated sinc filter, per (40), is as shown in (41).

$$H_{dec}[n,a] = H[nN,a] = \frac{1}{N^{M}} \sum_{j=0}^{Nn} \binom{M}{j-a}_{N-1} \tag{41}$$

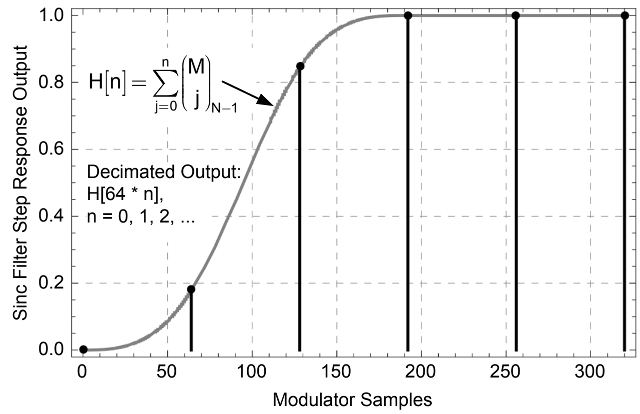

Fig. 3. Step response of a third-order sinc filter decimated every 64 samples (M = 3, N = 64). The curve is the output of the sinc filter at the modulator rate: (28) with a = 0. The individual points are the values of H[n] evaluated every 64th n.

V. Maximum Change in Value Between Two Consecutive Decimated Sinc Filter Output Samples

In linear time-invariant (LTI) systems, the impulse response is the derivative of the step response and, hence, the maximum value of the impulse response indicates the location of the maximum rate of change for the step response. Theorem 3.5 shows that this maximum rate of change must therefore occur at (14). The difference between two consecutive values of the decimated step response[6] is as shown in (42).

$$\begin{aligned} \Delta H_{dec}[x+1] &\equiv H_{dec}[x+1] - H[x] \\ &= \frac{1}{N^{M}} \sum_{j=0}^{N(x+1)} \binom{M}{j}_{N-1} - \frac{1}{N^{M}} \sum_{j=0}^{Nx} \binom{M}{j}_{N-1} \\ &= \frac{1}{N^{M}} \sum_{j=x(N+1)}^{Nx} \binom{M}{j}_{N-1} \\ &\text{for } x \in \mathbb{N} \end{aligned} \tag{42}$$

An example of the impulse response and step response for a third-order sinc filter with an oversample ratio of *N* = 128 is shown in Fig. 4.

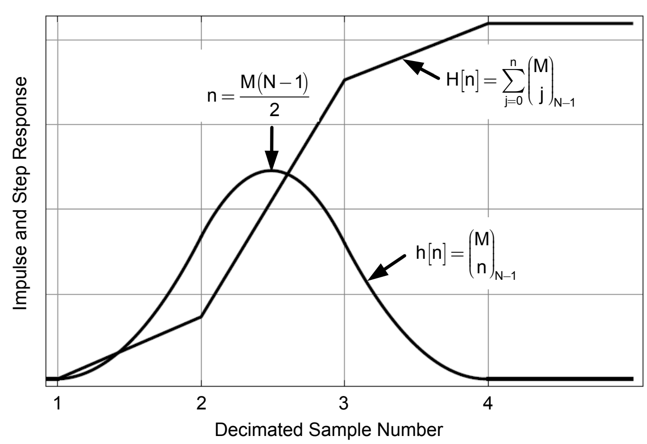

Fig. 4. Impulse response h[n] and step response H[n] for an example sinc filter (N = 128, M = 3). The time value corresponding to n = M(N – 1)/2 indicates the location of the maximum rate of change of the step response. (not drawn to scale.)

[6] Here, the step response "shift" factor a is neglected because it is a constant shift that does not affect the maximum change between consecutive samples.

TABLE I
MAXIMUM CHANGE IN VALUE BETWEEN TWO CONSECUTIVE SAMPLES OF DECIMATED SINC FILTER OUTPUT NORMALIZED TO FULL SCALE FOR VARIOUS M AND N CALCULATED FROM (43)

M	**N**												
	1	**2**	**4**	**8**	**16**	**32**	**64**	**128**	**256**	**512**	**1024**	**2048**	**4096**
1	1	1	1	1	1	1	1	1	1	1	1	1	1
2	1	1	0.875	0.813	0.781	0.766	0.758	0.754	0.752	0.751	0.750	0.750	0.750
3	1	0.750	0.688	0.672	0.668	0.667	0.667	0.667	0.667	0.667	0.667	0.667	0.667
4	1	0.875	0.727	0.661	0.629	0.614	0.606	0.603	0.601	0.600	0.599	0.599	0.599
5	1	0.625	0.566	0.554	0.551	0.550	0.550	0.550	0.550	0.550	0.550	0.550	0.550
6	1	0.781	0.631	0.568	0.534	0.525	0.518	0.514	0.513	0.512	0.511	0.511	0.511
7	1	0.547	0.494	0.483	0.480	0.480	0.479	0.479	0.479	0.479	0.479	0.479	0.479
8	1	0.711	0.565	0.506	0.479	0.466	0.459	0.456	0.454	0.454	0.453	0.453	0.453
9	1	0.492	0.444	0.434	0.431	0.431	0.430	0.430	0.430	0.430	0.430	0.430	0.430
10	1	0.656	0.516	0.460	0.435	0.423	0.417	0.414	0.412	0.412	0.411	0.411	0.411

It is trivial to show by symmetry and the unimodal / global maximum properties of the impulse response (Theorems 3.2 and 3.5) that the summation index for the maximum change in two consecutive decimated values must include M(N – 1)/2. For an oversample ratio *N*, then, the summation in (42) must range N/2 below the global maximum to N/2 above the global maximum. Note that M(N – 1)/2 may be non-integer when *N* is even. In this case, M(N – 1)/2 ± N/2 may also be non-integer. Thus, the upper limit of the summation must be rounded down and the lower limit rounded up, as shown in (43), the final expression for maximum change in consecutive samples.

$$\max_{n\in\mathbb{N}}\left(\Delta H_{dec}[n]\right)=\frac{1}{N^M}\sum_{j=\left\lceil \frac{M(N-1)}{2}-\frac{N}{2}\right\rceil}^{\left\lfloor \frac{M(N-1)}{2}+\frac{N}{2}\right\rfloor}\binom{M}{j}_{N-1} \tag{43}$$

Table I provides values generated from (43) for a common range of *M* and *N*.

Furthermore, the value of *a* (the time-shift of the input step function) that generates this maximum dV/dt can be calculated. Simply taking the lower index of the summation in (43) and determining the number of modulator samples it is away from a multiple of *N* shows how much to shift the input step function to achieve the maximum dV/dt:

$$a_{\max\ dV/dt}=N-\left(\left\lceil \frac{M(N-1)}{2}-\frac{N}{2}\right\rceil \bmod N\right) \tag{44}$$

VI. EXAMPLE OF SLEW RATE CALCULATION FOR A COMMERCIALLY AVAILABLE ΔΣ ADC

This section examines a specific third-order sinc filter contained in a commercially available ΔΣ ADC. The transfer function provided for the commercially available ADC is shown in (45), where *N* is the oversampling ratio.

$$H(z)=\left[\frac{1-z^{-N}}{1-z^{-1}}\right]^3 \tag{45}$$

With a fixed modulator clock of 1.024 MHz and an oversampling ratio of *N* = 64*,* the maximum change between two samples calculated by (43) is 66.675 %FS.

Fig. 5 graphs (43) versus the output data rate of the ADC (that is, versus *N*), which shows how the maximum change between two consecutive samples changes depending on the oversample ratio.

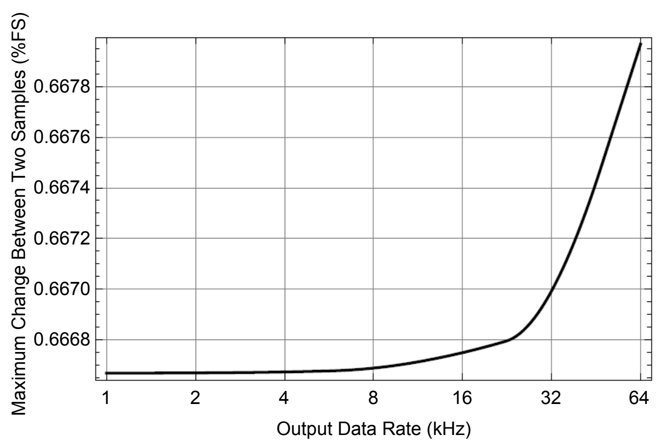

Fig. 5. Maximum change between two consecutive samples for commercially available ΔΣ ADC at various sample rates (dictating the oversample ratio *N*).

Using (44) to calculate for the 16 kHz case (N = 64) shows that the time shift on the input step function that causes the maximum dV/dt is as shown in (46).

$$\begin{aligned}a_{\max\ dV/dt}&=N-\left(\left\lceil \frac{M(N-1)}{2}-\frac{N}{2}\right\rceil \bmod N\right)\\&=64-\left(\left\lceil \frac{3(64-1)}{2}-\frac{64}{2}\right\rceil \bmod 64\right)\\&=2\end{aligned} \tag{46}$$

The decimated step response values, calculated using (41), are given in Table II.

TABLE II
VALUES OF ΔΣ ADC STEP RESPONSE THAT INCLUDE MAXIMUM dV/dt GENERATED FROM (41) FOR N = 64, M = 3, AND a = 2

Sample Number	Step Response Value	Change in Value dV/dt
0	0	0
1	$\frac{1365}{8192}$	$\frac{1365}{8192} \approx 0.16663$
2	$\frac{6827}{8192}$	$\frac{2731}{4096} \approx 0.66675$
3	1	$\frac{1365}{8192} \approx 0.16663$

VII. Other Sinc Filter Characteristics for a Specific Filter Configuration

Whereas the previously developed method compares individual discrete-time derivatives to a maximum threshold, sinc filters exhibit other characteristics involving combinations of discrete-time derivatives that can be reliably used for fault detection. This section continues to use the commercially available ΔΣ ADC containing a third-order sinc filter with an oversample rate of 64 with a full-scale range of $V_{ref} = \pm 2.4$ V.

A. *Fault Detection With Combination of Two Derivatives*

Examining the step response of the ADC's transfer function (45) shows that the geometric mean of two consecutive derivatives moving in the same direction is limited by some number x, as defined in (47).

$$\sqrt{\left(\left.\frac{dV}{dt}\right|_{t=n}\right)^2 + \left(\left.\frac{dV}{dt}\right|_{t=n-1}\right)^2} \le x \tag{47}$$

This must be the case because two consecutive derivatives in the same direction cannot both be too large and overshoot an ADC's full-scale range. Begin by setting the time-shift parameter $a = 0$ to give the step response shown in Fig. 6.

Table III shows the values from Fig. 6 along with the magnitude of the vector defined by two consecutive dV/dt values. As shown in Table III, the maximum value of the magnitude of the vector defined by two consecutive dV/dt values that have the same sign has a limit. By empirically exhaustive methods (i.e., generating a list of step responses for all possible time shifts $a \in [0,64]$) it can be determined that $a = 0$ produces the maximum magnitude value. Thus, the limit can be defined as shown in (48) (for the specific case of $N = 64$, $M = 3$).

$$\sqrt{\left(\left.\frac{dV}{dt}\right|_{t=n}\right)^2 + \left(\left.\frac{dV}{dt}\right|_{t=n-1}\right)^2} \le 0.6904 \cdot V_{ref} \tag{48}$$

Note that this limit is predicated on the assumption that $\left.\frac{dV}{dt}\right|_{t=n}$ and $\left.\frac{dV}{dt}\right|_{t=n-1}$ are both positive or both negative. A different expression, not calculated here, can be derived for cases where the two consecutive derivatives are of differing signs.

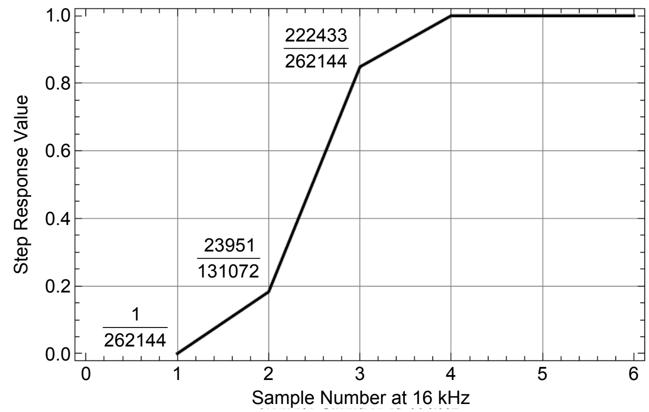

Fig. 6. Step response of commercially available ΔΣ ADC (N = 64, M = 3) running in 16 kHz mode with the time-shift factor $a = 0$.

A function generator was used to apply several different types of signals to the input of the commercially available ΔΣ ADC previously described: nearly full-scale square waves sweeping from 10 Hz to 8 kHz, sine waves sweeping from 10 Hz to 8 kHz, full-scale white noise, sawtooth waves, and so on. Approximately 1.6 million data points from the ADC output were recorded. Calculating the dV/dt for each set of samples and plotting the current dV/dt versus the previous one results in Fig. 7.

The maximum dV/dt limit boundary of (43) and the magnitude test of (48) are plotted as the thick black lines. All data points remain within the calculated limits. Note that the actual data contours in Quadrants I and III of Fig. 7 seem to indicate an actual limit somewhat closer to the origin than the limits calculated. It is speculated that this is due to the nonzero rise time of the function generator as well as the presence of a small resistor-capacitor (RC) filter at the input to the ADC being tested. These prevented the ADC from seeing a perfect step input.

TABLE III
VALUES OF STEP RESPONSE SHOWN IN FIG. 6 AND THE CORRESPONDING dV/dt VALUES

n	**h[n]**	$\left.\frac{dV}{dt}\right|_{t=n} = h[n] - h[n-1]$	$\sqrt{\left(\left.\frac{dV}{dt}\right|_{t=n}\right)^2 + \left(\left.\frac{dV}{dt}\right|_{t=n-1}\right)^2}$
0	0	0	NA
1	3.8147E–06	3.8147E–06	3.8147E–06
2	0.182731628	0.182727814	0.182727814
3	0.848514557	0.665782928	0.690403043
4	1	0.151485443	0.6827992

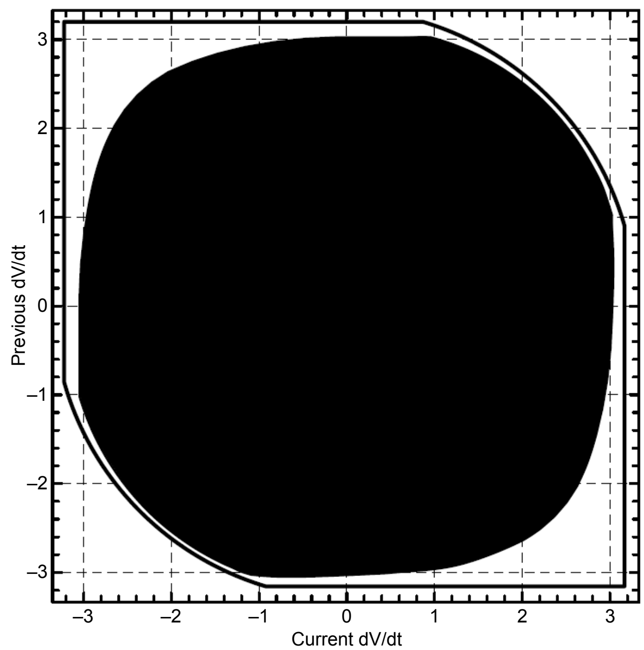

Fig. 7. Plot of the current difference between samples and the previous difference between samples for 1.6 million data points from a commercially available ΔΣ ADC. The plotted boundaries are a combination of the maximum dV/dt [= 66.675 %FS from (43)] and the maximum magnitude test from (48).

B. Fault Detection With a Combination of Three Derivatives

For a third-order sinc filter with an oversample ratio of 64, the geometric mean of any two derivatives of the same sign is limited. By examining how the step response of this sinc filter changes as the time shift of the input transient *a* varies from 0 to 64 (as shown in Fig. 8), a further limitation can be recognized.

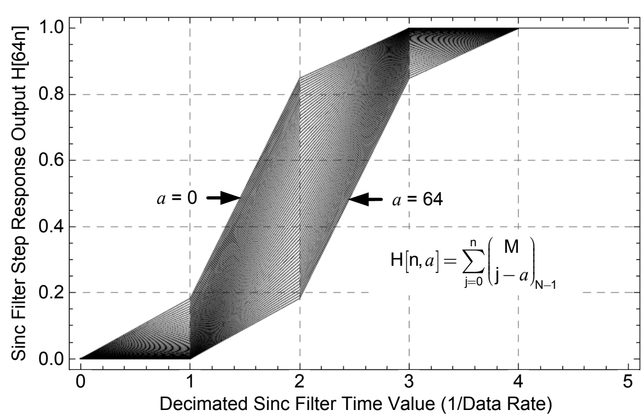

Fig. 8. Step response of commercially available ΔΣ ADC running in 16 kHz mode (oversample rate of 64). The parameter *a* (which is simply the time shift of the input step function) is varied from 0 to 64 to show how the decimated step response changes depending on when the input step transient occurs.

Assuming the sinc filter is completely "settled" (i.e., the filter's output is not changing), the derivative between n = 1 and n = 2 is inversely proportional to the previous derivative between n = 0 and n = 1. That is, when $\left.\frac{dV}{dt}\right|_{t=n-1}$ is small, $\left.\frac{dV}{dt}\right|_{t=n}$ cannot be as large as the maximum slew rate limitation calculated in (43). However, when $\left.\frac{dV}{dt}\right|_{t=n-1}$ is large enough, $\left.\frac{dV}{dt}\right|_{t=n}$ can be up to the filter's maximum limit.

When developing the error-checking technique, a derivative cannot simply be compared with the previous one because there is no indication of whether the filter is settled as predicated in Fig. 8. Thus, the sample prior to $\left.\frac{dV}{dt}\right|_{t=n-1}$ must be included. In the example of Fig. 8, this value is zero, resulting in (49).

$$\sqrt{\left(\left.\frac{dV}{dt}\right|_{t=n-1}\right)^2+\left(\left.\frac{dV}{dt}\right|_{t=n-2}\right)^2}=\left|\left.\frac{dV}{dt}\right|_{t=n-1}\right| \tag{49}$$

Note that $\left.\frac{dV}{dt}\right|_{t=n-1}$ can take many different values, depending on the time shift of the input step function set by *a*. Note also that this value defines a limit on the current dV/dt. However, for implementation purposes, look at the magnitude of the last two samples to ensure that this represents a settled value. Based on (42), this results in (50).

$$\left.\frac{dV}{dt}\right|_{t=1}=\frac{1}{N^M}\sum_{j=0}^{N}\binom{M}{j-a}_{N-1} \tag{50}$$

Plotting this value against the next derivative gives the curve shown in Fig. 9.

$$\left.\frac{dV}{dt}\right|_{t=2}=\frac{1}{N^M}\sum_{j=N}^{2N}\binom{M}{j-a}_{N-1} \quad \text{for } a\in[0,64] \tag{51}$$

Also plotted in Fig. 9 are the same data as shown in Fig. 7 with the magnitude of the previous two derivatives plotted on the horizontal axis and the magnitude of the current derivative on the vertical axis. Note that not one of the 1.6 million data points collected crosses the limit line.

By comparing the combination of three derivatives to the calculated limits, an error can be detected if the difference between two samples exceeds the limit line. Note that when the geometric mean of two previous derivatives is small, the maximum limit of the current derivative is also smaller than the maximum limit calculated by (43). This may produce tighter limits, allowing more subtle errors to be detected.

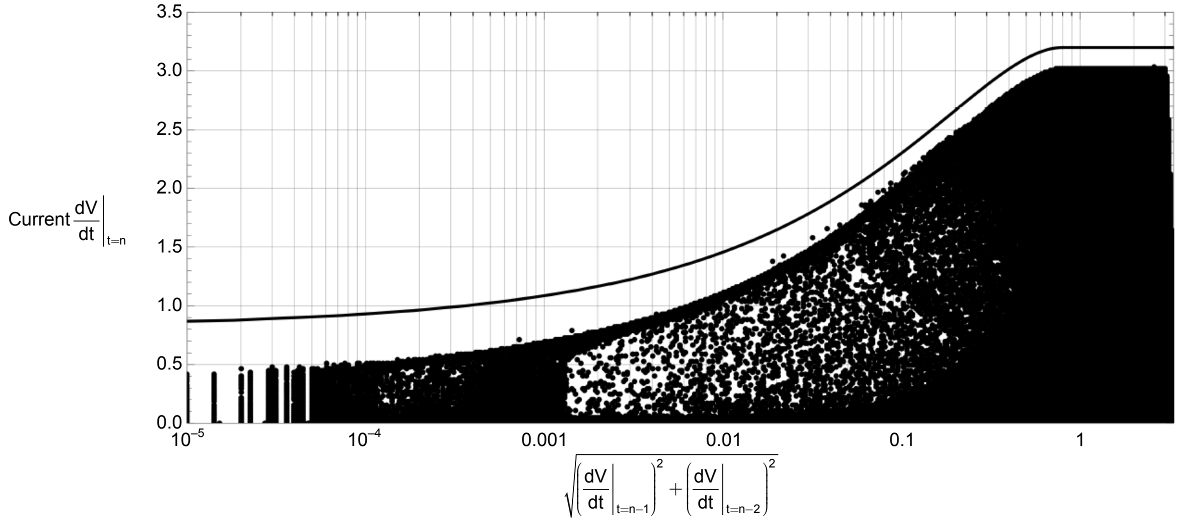

Fig. 9. Plot of 1.6 million data points from a commercially available ΔΣ ADC. The limit line is described by (51) plotted as vertical values against (50) on the horizontal axis for $a \in [0,64]$.

VIII. Conclusion

Oversampling ΔΣ ADCs offer unparalleled accuracy and precision. The oversampling ADC topology necessitates that digital filtering be implemented to noise shape and decimation. The digital filter latency can be a barrier to multiplexing in test signals to verify the ADC health. A rudimentary verification of the ADC's integrity can be determined by comparing data from the ADC with known filter characteristics. The internal sinc-shaped filters common to ΔΣ ADCs exhibit a limited output swing characteristic. That is, the derivative of samples from a sinc filter has a finite limit that can be calculated. In addition, combinations of these derivatives can be used to discern data conformance to other filter characteristics. This paper demonstrates, by calculation and test results, an error-checking method for ΔΣ ADCs that is simple to implement.

Further work in this area may include developing the error-checking methods for the combination of two and three derivatives in a general case for a sinc filter of an arbitrary order and oversample ratio.

IX. References

[1] Y. Mukuda, Y. Ozawa, and M. Murano. *Method and apparatus for detecting abnormality in analog-to-digital converter*. U.S. Patent 5,432,514. 1995.

[2] J. M. Kasson and M. H. Graham. *Signal injection technique*. U.S. Patent 4,187,466. 1980.

[3] A. S. Willsky, "A Survey of Design Methods for Failure Detection in Dynamic Systems," *Automatica*, Vol. 12, 1976, pp. 601–611.

[4] J. Candy, "Decimation for Sigma Delta Modulation," *IEEE Transactions on Communications*, Vol. 34, Issue 1, January 1986, pp. 72–76.

[5] M. J. M. Pelgrom, *Analog-to-Digital Conversion*. Springer, New York, NY, 2010.

[6] R. J. Baker, *CMOS: Mixed-Signal Circuit Design*. Wiley-IEEE Press, Piscataway, NJ, 2009.

[7] T. C. Mallett, "Systems and Methods for Identifying a Failure in an Analog to Digital Converter." U.S. Patent Application US14802787, filed July 17, 2015.

[8] M. R. Spiegel, S. Lipschutz, and J. Liu, *Mathematical Handbook of Formulas and Tables, 4th ed*. McGraw-Hill Companies, Inc., New York, NY, 2009.

[9] J. A. Rodríguez, "Polynomial Raised to the Arbitrary Exponent, Villareal Method," *Soft Jar Mathematical Notes,* 2009. Available: http://www.soft-jar.ucoz.com.

[10] L. Euler. "On the Expansion of the Power of Any Polynomial $1 + x + x^2 + x^3 + x^4 +$ etc," *Nova Acta Academiae Scientarum Imperialis Petropolitinae 12*, 1801, pp. 47–57.

[11] H. Belbachir, S. Bouroubi, and A. Khelladi, "Connection Between Ordinary Multinomials, Generalized Fibonacci Numbers, Partial Bell Partition Polynomials and Convolution Powers of Discrete Uniform Distribution," *arXiv*, August 2007.

[12] E. Hogenauer, "An Economical Class of Digital Filters for Decimation and Interpolation," *IEEE Transactions on Acoustics, Speech, and Signal Processing*, Vol. 29, Issue 2, April 1981, pp. 155–162.

[13] R. P. Stanley, "Log-Concave and Unimodal Sequences in Algebra, Combinatorics, and Geometry," *Annals of the New York Academy of Sciences*, Vol. 576, December 1989, pp. 500–535.

[14] A. V. Oppenheim and R. W. Schafer, *Discrete-Time Signal Processing*. Prentice Hall, Upper Saddle River, NJ, 2009.

[15] B. P. Lathi, *Linear Systems and Signals*. Oxford University Press, New York, NY, 2004.

[16] J. C. Candy and G. C. Temes, *Oversampling Delta-Sigma Data Converters: Theory, Design, and Simulation*. Wiley-IEEE Press, New York, NY, 1992.

[17] R. Schreier and G. C. Temes, *Understanding Delta-Sigma Data Converters*, Wiley-IEEE Press, Hoboken, NJ, 2005.

X. Biography

Travis C. Mallett received a B.S. degree in electrical engineering *cum laude* from the WSU Honors College at Washington State University, Pullman, WA, USA in 2014. He also received a B.S. degree in General Studies, General Mathematics *cum laude*, and a B.A. degree in Music *cum laude* from Washington State University in 2014. He has been with Schweitzer Engineering Laboratories, Inc. in Pullman, WA since 2008 and is currently a hardware engineer with the Distribution Engineering group in power systems infrastructure. His fields of interest include analog and mixed-signal circuit design.

20171020 • TP6776-01